Supplementary Discussion

Structural determination of CusBA

Data collection and refinement statistics are summarized in Table S1. The resulting experimental electron density maps based on MRSAD (Fig. S1) reveal that the asymmetric unit consists of one CusA and two CusB protomers. The native crystal structure of CusBA was then resolved to a resolution of 2.90 Å (Table S1). The final structure includes 93% of the total amino acids, and is refined to R_{work} and R_{free} of 22.9% and 26.7%, respectively.

Overall conformations of the CusA and CusB protomers

The overall conformation of the CusA protomer in the complex resembles the previously determined apo-CusA structure.[1] Superimposition of these two structures results in an RMSD of only 1.0 Å for 1,019 C^{α} atoms. For the CusB protomers, two distinct conformations of this adaptor are captured in the complex. When we superimpose these two elongated protein structures a high RMSD of 7.5 Å is observed for the 321 C^{α} atoms, suggesting that the conformations of these two protomers are quite different. Interestingly, a comparison of these two molecules with the two previously determined structures[2] of CusB indicates that the four molecules display four distinct conformations, presumably representing different transient states of this membrane fusion protein (Fig. S4). This observation is consistent with the previous finding that these membrane fusion proteins are highly flexible,[2,17,18] with the ability to change their conformations after ligand binding.[23,34] Indeed, it has been demonstrated that binding of

metal ions trigger significant conformational changes in the CusB[23] and ZneB[34] adaptor proteins.

Results of the ITC experiment

As mentioned in the text, the ITC data indicates an equilibrium dissociation constant of 5.1 ± 0.3 μM. The titration is characterized by a negative enthalpic contribution (ΔH = -22.4 ± 0.3 kcal/mol), which yields a hyperbolic binding curve (Fig. S2). The entropic contribution (ΔS) of this binding reaction was found to be -50.9 cal•mol^{-1}•deg^{-1}. Interestingly, the molecular ratio for this binding reaction based on ITC is one CusA monomer per two CusB protomers, although it is known that ITC cannot be used to precisely determine the molar ratio. This result is indeed confirmed by the crystal structure where each protomer of CusA binds two molecules of CusB.

Inhibition of the pump

Recently, artificial peptides, DARPins, have been introduced to bind and effectively inhibit the AcrB transporter.[11] The inhibitor-binding site is found right above the cleft formed between PC1 and PC2 of AcrB.[11] Interestingly, the location of this inhibitor-binding site corresponds to the binding site for molecule 2 of CusB in the CusBA complex. Thus, it is likely that the mechanism of action for these inhibitors may be the disruption of the adaptor-transporter interaction by competition. If this is the case, then a proposed $AcrB_3$-$AcrA_3$-$TolC_3$ model[18] containing only one protomer of AcrA per AcrB protomer would not be sufficient to form a functional pump. However, there is a possibility that the two sub-families of these RND transporters may operate differently.

The 2:1 adaptor-to-transporter stoichiometry may only apply to the heavy-metal efflux systems. Nonetheless, the hexameric arrangement of these membrane fusion proteins has also been observed in the crystal structure of MacA in which six protomers assemble to create a large channel.[35]

The predicted $CusC_3$-$CusB_6$-$CusA_3$ model

The predicted CusC structure is indeed reminiscent of the OprM trimer, indicating that the trimeric CusC channel consists of a membrane-anchoring β-barrel domain and a periplasmic α-helical tunnel. The periplasmic tunnel is about 100 Å long with an outer diameter of 39 Å at the tip of the tunnel. As the inner diameter of the top portion of the hexameric CusB channel is larger than the outer diameter of the periplasmic end of the trimeric CusC channel, this suggests that the CusC channel could easily be inserted into the CusB channel when they contact one another. After optimizing this docked model, the final structure of the CusCBA complex suggests that CusC interacts with CusBA at the interior of the upper half of the channel formed by the α-helical domain (Domain 4) of CusB, primarily through coiled-coil interactions (Fig. S3a).

Genetic experiments revealed that the α-helical domain of the TolC channel is mapped predominantly to the β-barrel domain of the AcrA adaptor.[24] This result has led to the hypothesis that the MexA adaptor provides two binding sites for the periplasmic α-helices of the OprM channel, one at the α-hairpin domain and the other at the β-barrel domain.[20] These two domains should correspond to Domain 4 and Domain 2 of CusB, respectively. It is likely that the above docked CusCBA structure is a useful snapshot for how CusBA recruits CusC at the early stage. To pump metal ions, the CusC channel may

need to contact the top of CusA. Interestingly, the CusBA crystal structure suggests that the funnel top of the trimeric CusA pump is surrounded with Domain 2 of the CusB hexamer. Thus, it is likely that the funnel top of CusA, α-helical end of CusC, and Domain 2 of CusB may contact one another during the extrusion cycle (Fig. S3b). If this is the case, it is possible that the recruitment of the CusC channel to the tripartite complex is a two-stage process. The first step might involve an interaction between both the α-helical domains of CusB and CusC. Then, the CusC channel could slide further down the CusB channel and contact the top of CusA whereas this region is surrounded with Domain 2 of the CusB hexamer (Fig. S3).

References

34. De Angelis, F., Lee, J. K., O'Connell III, J. D., Miercke, L. J. W., Verschueren, K. H., Srinivasan, V., Bauvois, C., Govaerts. C., Robbins, R. A., Ruysschaert, J.-M., Stroud, R. M. & Vandenbussche, G. Metal-induced conformational changes in ZneB suggest an active role of membrane fusion proteins in efflux resistance systems. *Proc. Natl. Acad. Sci. USA* **107,** 11038-11043 (2010).

35. Yum, S., Xu, Y., Piao, S., Sim, S.-H., Kim, H.-M. Jo, W.-S., Kim, K.-J., Kweon, H.-S., Jeong, M.-H., Lee, K. & Ha, N.-C. Crystal structure of the periplasmic component of a tripartite macrolide-specific efflux pump. *J. Mol. Biol.* **387,** 1286-1297 (2009).

Supplemental Figures

Fig. S1. Stereo view of the experimental electron density map at a resolution of 2.9 Å. (a) Anomalous maps of the 12 selenium sites (contoured at 4 σ). The selenium sites corresponding to the six methionines from molecule 1 of CusB and another six methionines from molecule 2 of CusB are in red. The Cα traces of CusA, and molecules 1 and 2 of CusB are in yellow, green and cyan, respectively. (b) Representative section of the electron density at the junction of the CusA and CusB molecules. The electron density (colored white) is contoured at the 1.2 σ level and superimposed with the final refined model (yellow, CusA; green, molecule 1 of CusB; cyan, molecule 2 of CusB).

Fig. S2. Representative isothermal titration calorimetry for the binding of CusB to CusA. (a) Each peak corresponds to the injection of 10 μl of 350 μM CusB in buffer containing 20 mM Na-phosphate (pH 7.5) and 0.05% CYMAL-6 into the reaction cell containing 14 μM CusA in the same buffer. (b) Cumulative heat of reaction is displayed as a function of the injection number. The solid line is the least-square fit to the experimental data, giving a K_D of 5.1 ± 0.3 μM. The molar-to-molar ratio of CusA (monomer):CusB (monomer) is 1:2.

Fig. S3. Docking of CusC to CusBA. (a) The α-helical end of CusC interacts with the α-helices (Domain 4) of CusB in the CusBA complex. (b) The funnel top of CusA, α-helical end of CusC and Domain 2 of CusB contact one another when the CusC channel slides further down the hexameric CusB channel. The surface rendering of the $CusC_3$-

$CusB_6$-$CusA_3$ complex is colored as follows: green, CusC trimer; blue, CusB hexamer; red, CusA trimer.

Fig. S4. Comparsion of the four conformations of CusB observed in the CusBA and CusB crystals. This superimposition suggests that the main difference between the conformations of these four CusB molecules comes from Domains 1 and 2 (red, molecule 1 of CusB in the CusBA co-crystal structure; blue, molecule 2 of CusB in the CusBA co-crystal structure; green, molecule A of CusB in the CusB crystal structure; orange, molecule B of CusB in the CusB crystal structure).

Table S1. Data collection and refinement statistics of the CusBA complex.

	CusA (Native)-CusB (Native)	CusA (Native)-CusB (SeMet)
Data collection		
Space group	*R*32	*R*32
Cell dimensions		
a, *b*, *c* (Å)	160.24, 160.24, 682.69	160.41, 160.41, 682.03
α, β, γ (°)	90, 90, 120	90, 90, 120
Wavelength	0.9791	0.9791
Resolution (Å)	40-2.90 (3.00-2.90)	40-4.23 (4.38-4.23)
R_{sym} or R_{merge}	9.0 (45.6)	9.0 (36.6)
$I/\sigma I$	9.7 (1.5)	6.3 (3.3)
Completeness (%)	92.4 (90.4)	91.1 (90.7)
Refinement		
Resolution (Å)	40-2.90	
No. reflections	56,651	
$R_{work/}$ R_{free}	0.229/0.267	
No. atoms		
Protein	12,854	
Ligand/ion	0	
Water	19	
B-factors		
Protein	68.12	
Ligand/ion		
Water	42.06	
R.m.s deviations		
Bond lengths (Å)	0.003	
Bond angles (°)	0.683	

*Highest resolution shell is shown in parenthesis.

Figure S1a

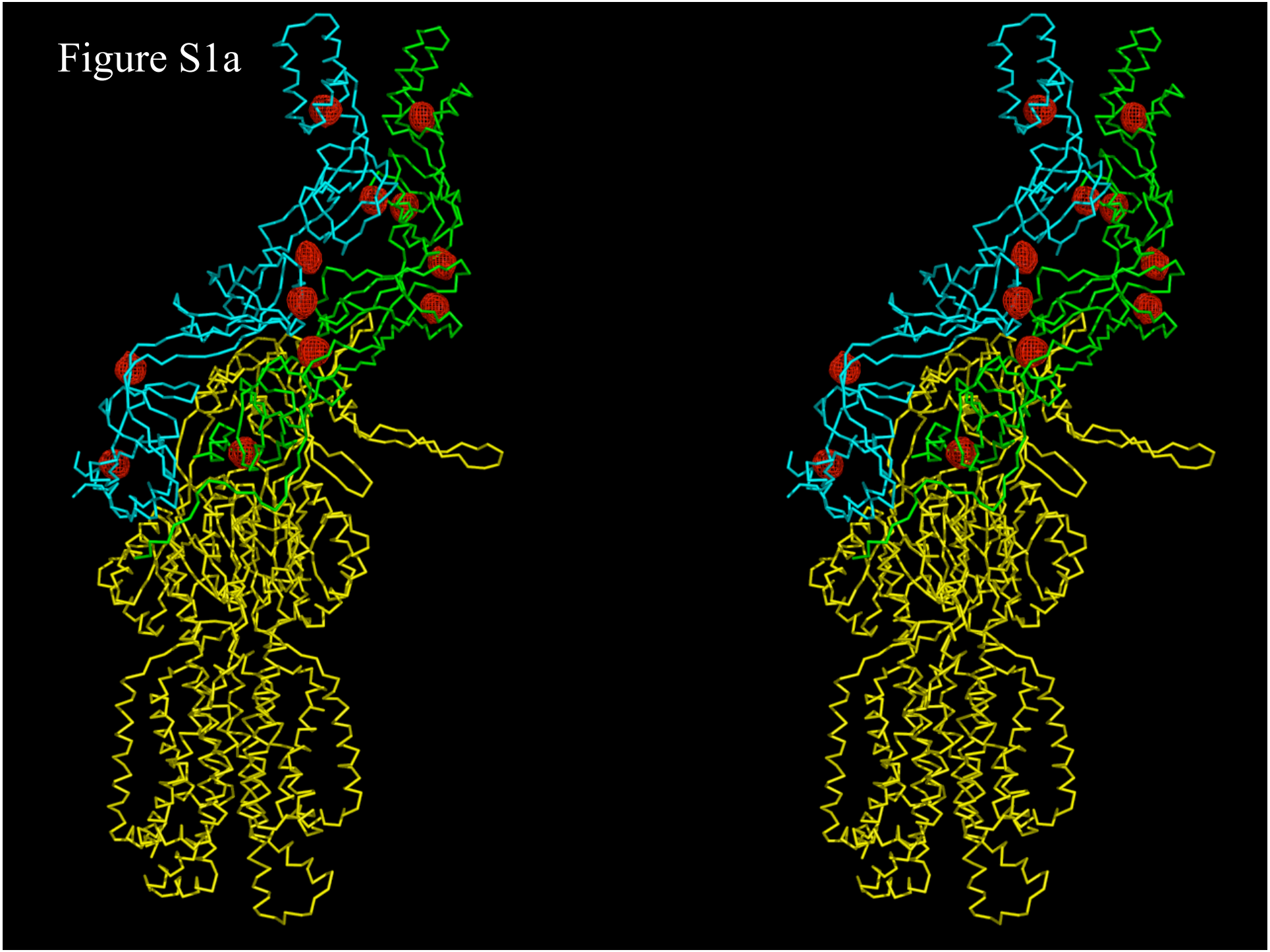

Figure S1b

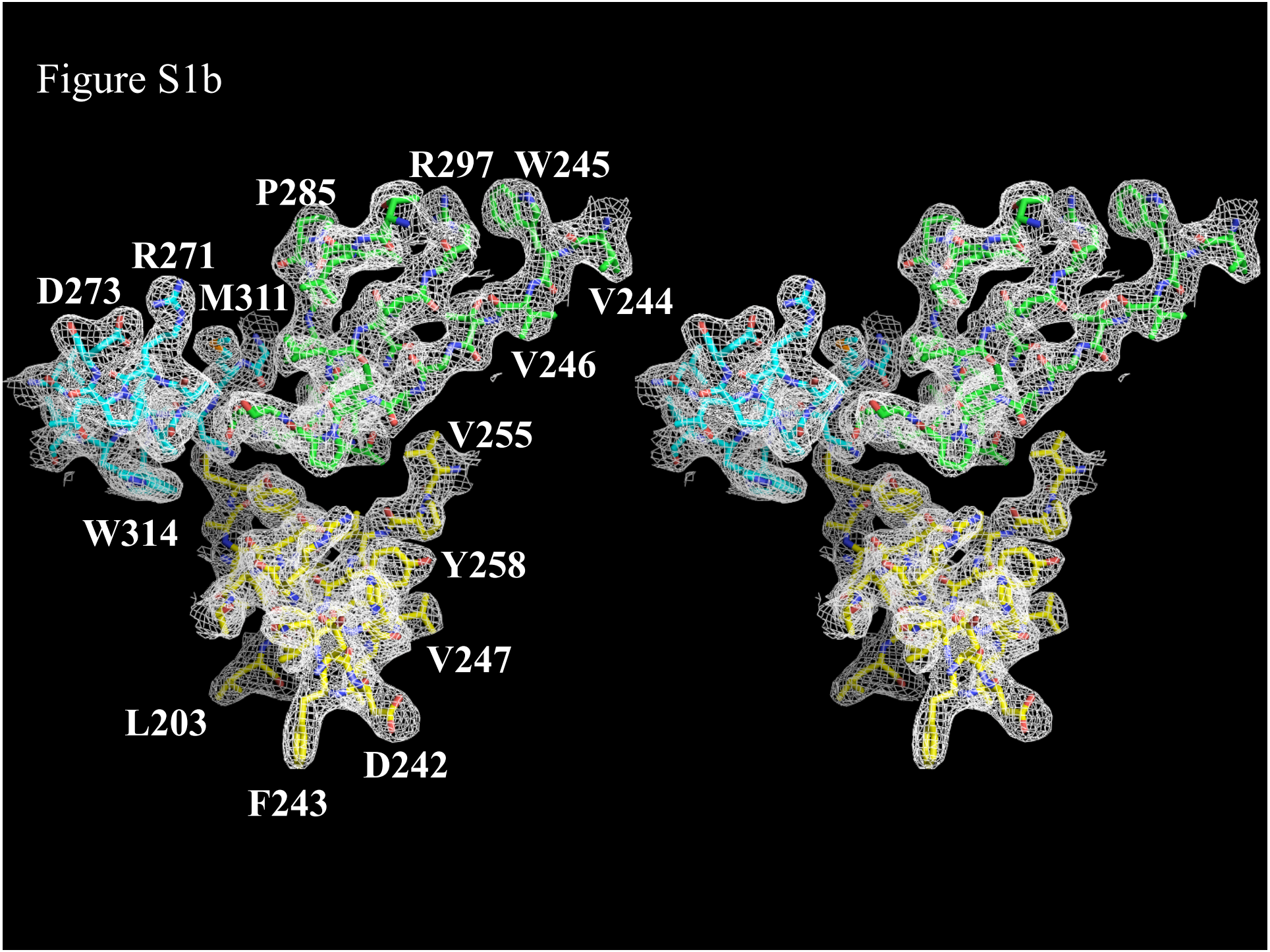
R297
W245
P285
R271
D273
M311
V244
V246
V255
W314
Y258
V247
L203
D242
F243

Figure S2

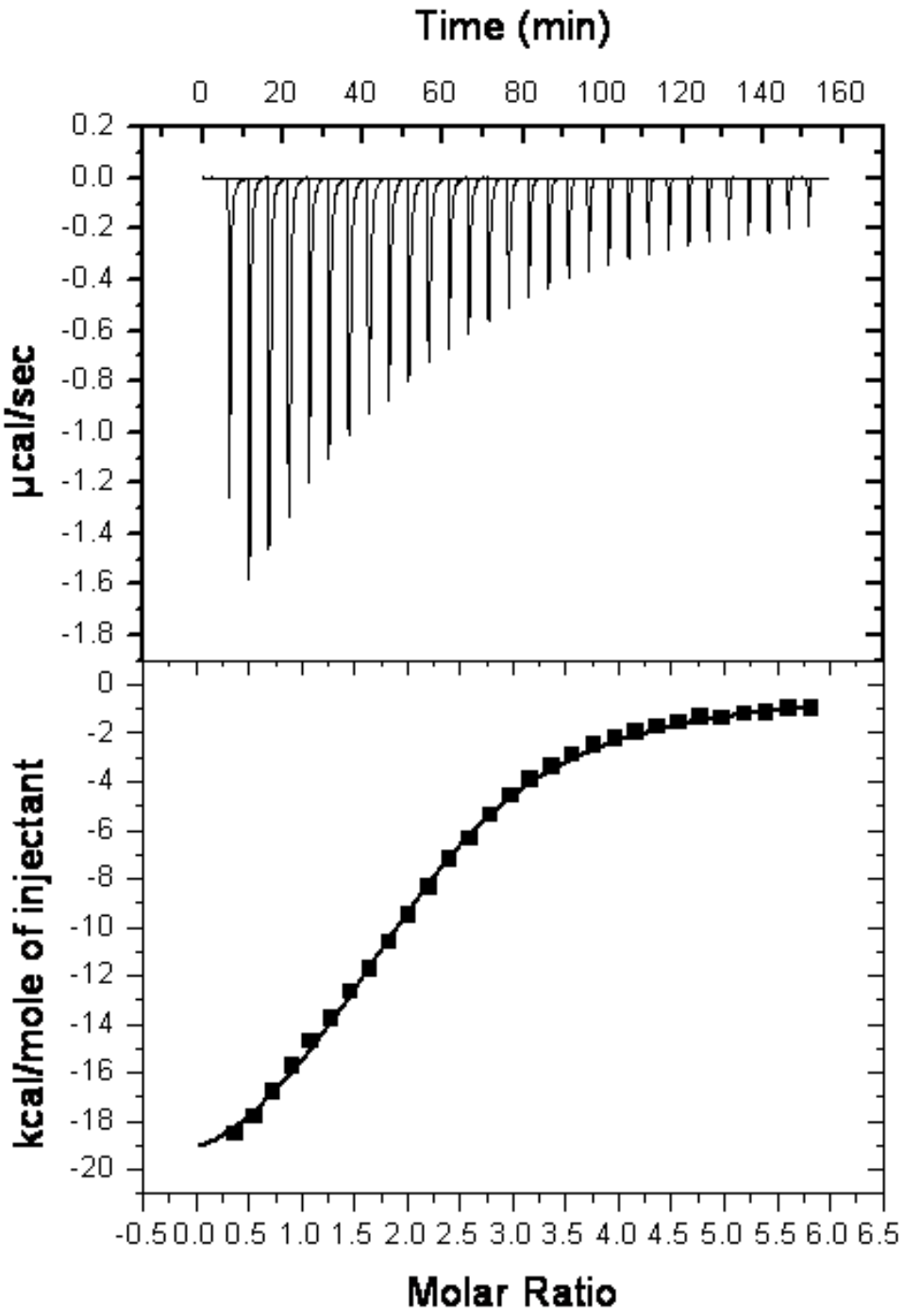
Time (min)
0 20 40 60 80 100 120 140 160
0.2
0.0
-0.2
-0.4
-0.6
-0.8
-1.0
-1.2
-1.4
-1.6
-1.8
µcal/sec
0
-2
-4
-6
-8
-10
-12
-14
-16
-18
-20
kcal/mole of injectant
-0.5 0.0 0.5 1.0 1.5 2.0 2.5 3.0 3.5 4.0 4.5 5.0 5.5 6.0 6.5
Molar Ratio

Figure S3

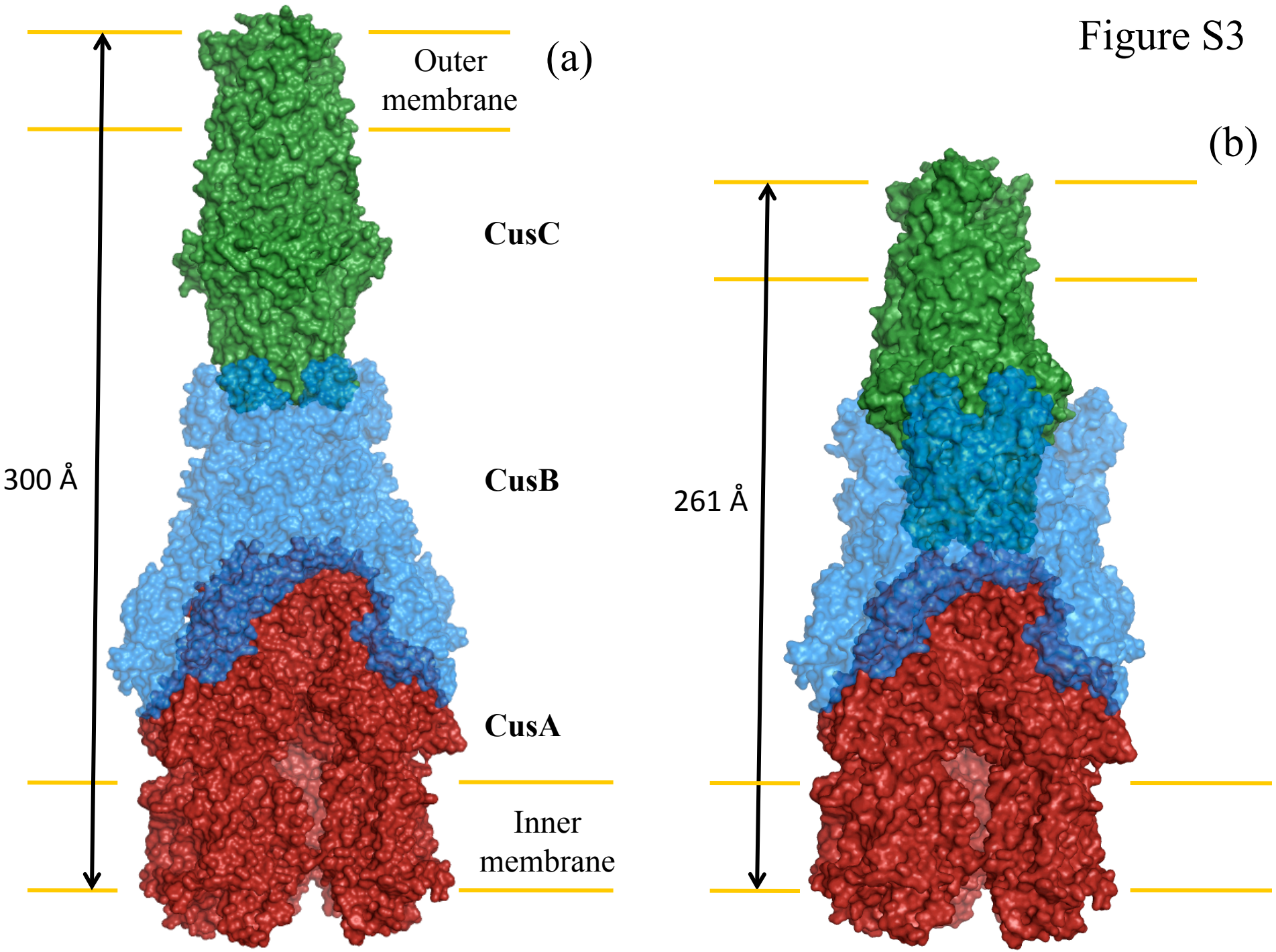

Figure S4